

Acoustoelectric current transport through single-walled carbon nanotubes

J. Ebbecke,^{1,*} C. J. Strobl,² and A. Wixforth¹

¹*Institut für Physik der Universität Augsburg, Experimentalphysik I, Universitätsstrasse 1, 86135 Augsburg, Germany*

²*Sektion Physik der Ludwig-Maximilians-Universität and Center for NanoScience (CeNS), Geschwister-Scholl-Platz 1, 80539 Munich, Germany*

(Received 14 May 2004; revised manuscript received 5 August 2004; published 3 December 2004)

We have contacted single-walled carbon nanotubes after aligning the tubes by the use of surface acoustic waves. The acoustoelectric current has been measured at 4.2 K, and a probing of the low-dimensional electronic states by the surface acoustic wave has been detected. By decreasing the acoustic wavelength resulting in an adjustment to the length of the defined carbon nanotube constriction, a quantization of the acoustoelectric current has been observed.

DOI: 10.1103/PhysRevB.70.233401

PACS number(s): 73.63.Kv, 72.50.+b, 73.23.Hk, 85.35.Kt

Due to their remarkable electrical and mechanical properties, carbon nanotubes (CNT's) have become an important field of research since their discovery in 1991 (Ref. 1). They can be synthesized as single-walled carbon nanotubes (SWNT's) as well as multiwalled carbon nanotubes (MWNT's). Because of their small diameter of around 1 nm and a length of up to several micrometers SWNT's are by definition an ideal one-dimensional electronic system. Efforts have been made to investigate fundamental one-dimensional effects like Luttinger liquid behavior.² Also by contacting the CNT's with metal leads zero-dimensional electronic systems can be designed³⁻⁹ with a length between a micrometer and several tens of nanometers and they have revealed an increased zero-dimensional confinement in comparison with their semiconductor counterparts of the same length.

In this paper, we report on the observation of an acoustoelectric current transport through carbon nanotube constrictions (CNTC's). For large wavelengths of the surface acoustic wave (SAW) the current oscillates by increasing the SAW amplitude, which exhibits a probing of the low-dimensional electronic states. By adjusting the acoustic wavelength to the length of the CNTC the acoustoelectric current becomes quantized for certain SAW amplitudes. At first sight, these results resemble the proposed quantized adiabatic charge transport in CNT's of Ref. 10. There, the potential of the SAW is assumed to induce a miniband spectrum in the CNT's and an adiabatic quantized transport as described by Thouless¹¹ is suggested. But in contrast to this mechanism here a turnstilelike modulation of the tunneling barriers by the piezoelectric potential of the SAW is assumed to cause the acoustoelectric current quantization. Also beside the fact that Coulomb repulsion is likely to be important for the current quantization the results presented in this paper are in close relation to the proposed carbon nanotube electron pump.¹²

Two sets of samples have been processed almost solely by optical lithography and results will be presented exemplarily for one sample of each set (in the following named sample A and sample B). The only difference is the periodicity of the interdigital transducers (IDT's). On sample A, first two IDT's with a periodicity of 35 μm have been processed on LiNbO₃ substrate (rotation 128° Y-cut X propagation) by optical li-

thography. At a sound velocity of the SAW of $v=3850$ m/s (at $T=4.2$ K) the resonance frequency of the transducers is given by $f_1=v/p=110$ MHz. On sample B, two IDT's have been defined by *e*-beam lithography with a periodicity of 8.1 μm , resulting in a primary frequency of $f_1=475$ MHz. SWNT's grown by an arc discharge method have been suspended in water with 1 wt % sodium-dodecylsulfate (SDS). The suspension was subjected to ultrasonic agitation for 10 min and then centrifuged at 10 000 g for 10 min to remove larger particles. Small drops of the liquid have been dispensed between the transducers and glass plates have been placed above. A SAW launched with one of the IDT's has two effects. First the parallel component of its piezoelectric field aligns the NT's in parallel to the wave vector of the SAW. Second, the transversal component of the crystal particle movement induces strong fluidic processes in the liquid. The superposition of both effects is an alignment of the NT's with an angle between 25° and 45° with respect to the propagation direction of the SAW. This process of aligning NT's has been described in detail in Ref. 13 where MWNT's have been aligned. In Fig. 1(a) an atomic force microscope (AFM) picture of short aligned SWNT's is shown. The nanotubes are aligned with an angle of $\pm 45^\circ$ with respect to the traveling wave. After cleaning the samples by rinsing them in de-

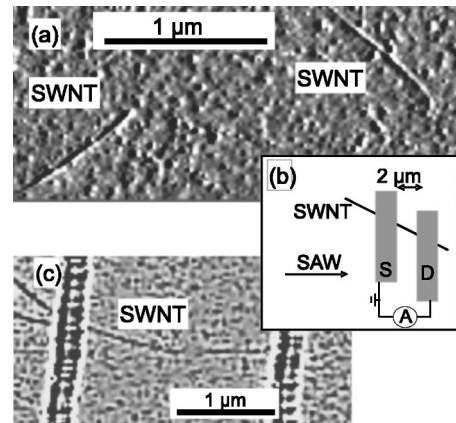


FIG. 1. (a) AFM picture of two short SWNT's aligned by the SAW at $\pm 45^\circ$. (b) Schematic sample layout. (c) AFM picture of a contacted SWNT of sample A.

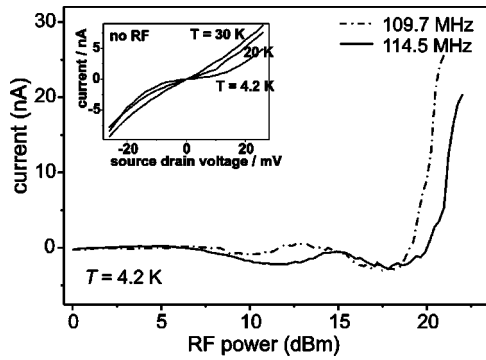


FIG. 2. Sample A: acoustoelectric current oscillations by raising the applied rf power for two frequencies inside the passband of the IDT. Source-drain measurements for different temperatures are shown as an inset.

ionized water and drying with nitrogen gas pairs of metal contacts have been processed where the drops of SWNT suspension had been [see schematic sample layout given in Fig. 1(b)]. The contacts are metal fingers of 30-nm-thick titanium with a length of $600 \mu\text{m}$ and a width of $2 \mu\text{m}$. The gap between the contact pair is also $2 \mu\text{m}$ so that the contacted SWNT's have a length between $2.2 \mu\text{m}$ and $2.8 \mu\text{m}$ depending on the alignment angle between 25° and 45° . An AFM picture of a contacted SWNT of sample A is shown in Fig. 1(c). All measurements have been carried out in a variable-temperature cryostat with base temperature of $T=4.2 \text{ K}$.

First, investigations made with sample A will be presented. The two-terminal resistance of the device at room temperature was $500 \text{ K}\Omega$. By using the sample holder as a back gate no change in conductance has been detected for voltages of $V_{BG}=\pm 20 \text{ V}$ at room temperature (also for sample B). Consequently we assume the contacted CNT's to be metallic. The current transport through the SWNT has been detected using a Keithley 2400 SourceMeter as a function of applied source drain voltage for temperatures between $T=4.2 \text{ K}$ and $T=30 \text{ K}$ (inset of Fig. 2). At $T=4.2 \text{ K}$ a clear nonlinearity has been measured that has almost disappeared at $T=30 \text{ K}$. The expected Coulomb blockade behavior is masked by the vanishing conduction of the contacts to the CNT and the capacitance of the back gate is too small to be used in this case. In Ref. 8 a value of the charging energy of a CNT quantum dot with $1.3 \mu\text{m}$ length has been measured to be $E_C=6 \text{ meV}$. With the estimation of a linear dependence of the capacity on the length of the CNT a value of $E_C\approx 3 \text{ meV}$ can be assumed for the CNTC's presented here. Due to the fact that we cannot verify any Coulomb oscillations because of the lack of a gate and also that a $2\text{-}\mu\text{m}$ -long constriction with a diameter of a few nanometers is venturous to term a zero-dimensional quantum dot, we name our devices CNT constrictions but still in mind that the CNTC have well-defined electronic states.

Two measurements of the acoustoelectric current as a function of applied rf power are shown in Fig. 2 for two different frequencies inside the passband of the IDT's of sample A (using a Keithley 617 electrometer and a Rohde-Schwarz signal generator SMP2). The piezoelectric field of the SAW transmits a momentum to the electrons in the

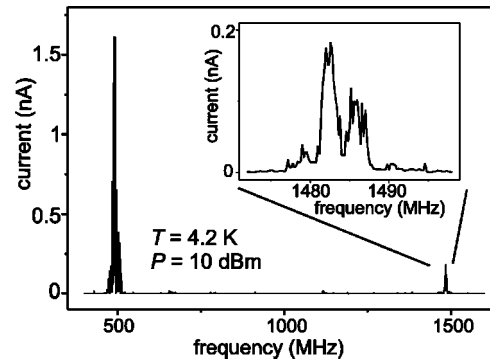


FIG. 3. Sample B: acoustoelectric current as a function of applied rf frequency. The inset shows an enlargement of the current at the frequency of the third harmonic.

SWNT and an acoustoelectric current can be detected. By raising the rf power—meaning an increase of the SAW amplitude—the acoustoelectric current through the CNTC is oscillating for both frequencies used. The horizontal shift in rf power of the current minima is caused by the fact that the transducer is effective differently in launching a SAW at these two frequencies. After finishing the measurements and taking the figure of a contacted CNT [see Fig. 1(c)] we placed sample A for 30 s into an oxygen plasma. No conductivity of sample A has been detected afterwards.

In the following, experiments made with sample B will be presented. IDT's have been processed with a periodicity of $8.1 \mu\text{m}$, meaning an adjustment of the acoustic wavelength to the length of the CNTC. The acoustoelectric current transport through a SWNT as a function of applied rf frequency is shown in Fig. 3. Around the resonance frequency $f_1=475 \text{ MHz}$ an acoustoelectric current has been measured. But in addition to this signal at f_1 , another peak of the acoustoelectric current exists at a frequency of approximately $f_3=1480 \text{ MHz}$, which is slightly higher than the theoretical value of the third harmonic, $f_{3\text{theo}}=1425 \text{ MHz}$. This SAW launched by the same IDT has a wavelength of approximately $2.6 \mu\text{m}$. The two-terminal resistance of sample B at room temperature was $6.5 \text{ M}\Omega$ and therefore significantly higher than the resistance of sample A. This increase in resistance is caused by less effective electrical contacts to the SWNT resulting in a suppression of current transport at $T=4.2 \text{ K}$ in the interval of $\pm 2 \text{ V}$ source drain bias. Due to the lack of any appropriate gate (like in sample A), the charging energy of the CNTC could not be determined.

In Fig. 4 two measurements of the acoustoelectric current as a function of applied rf frequency are shown. The solid graph has been measured at a frequency inside the passband of the IDT's first harmonic and the other graph with a frequency of the IDT's third harmonic. For both frequencies the acoustoelectric current is zero for low rf power levels. By raising the rf power resulting in a launched SAW with larger amplitude the current increases until a plateau is reached. As a verification of the occurrence of plateaus the numerical derivative of the current is shown in the inset of Fig. 4 where the pronounced minima indicate the plateaus. At these rf power levels the acoustoelectric current is quantized. The rf levels at which plateaus occur are different for the two fre-

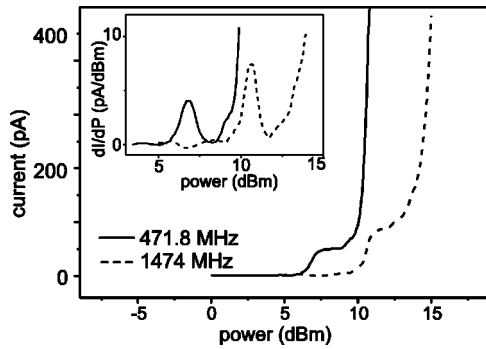


FIG. 4. Quantized acoustoelectric current as a function of applied rf power for two different SAW frequencies (first and third harmonics of the IDT) at 4.2 K. The upper graph shows the derivative of the current.

frequencies because the IDT is effective differently in launching the first and third harmonics (see Fig. 3). By further increasing the rf power the current also increase rapidly without showing any further well-quantized levels that could be caused by SAW-induced thermal heating. The piezoelectric potential at a rf power of $P=10$ dBm can be estimated using a simple model¹⁴ to be approximately a couple of 100 meV, meaning an effective heating of the sample.

A feature of this current quantization remaining to be explained is the value of the current plateaus. For the higher frequency the plateau value is $I=91$ pA, in contrast to the expected value of $I_3=ef_3=236$ pA, and for the lower frequency the quantized value is $I=49$ pA, where the theoretical current should be $I_1=ef_1=75$ pA. Although the current value on the shoulder visible next to the plateau for $f=471.8$ MHz (also visible as a shoulder in the derivative in the inset of Fig. 4) is $I=76$ pA $\approx ef_1$, no pronounced current quantization at $I=ef$ has been detected. In order to emphasize that these quantized acoustoelectric current values are not random, a statistic of all measured first plateau current values are given in Fig. 5. The values of both the first and third harmonics are shown in the same figure. The open squares are belonging to the lower frequency f_1 and their average value is $I_{average}=45$ pA, which is 60% of $I=ef_1$. The solid squares are associated with the third harmonic f_3 with an average current of $I_{average}=91$ pA, which is 40% of I

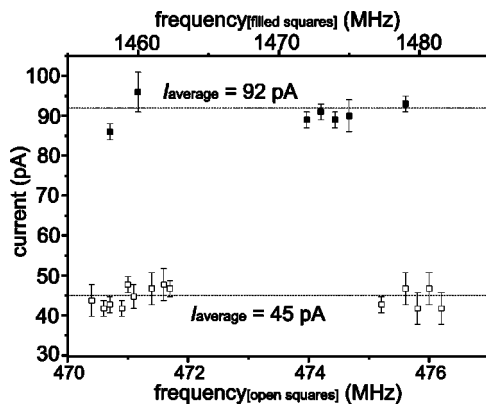


FIG. 5. Statistical overview of the height of the first current plateaus as a function of frequency.

$=ef_3$. A similar “fractional” plateau has been presented in Ref. 15 for quantized acoustoelectric current transport measurements through an unintentional quantum dot defined in a AlGaAs/GaAs heterostructure. We assume that some of the electrons are excited during the transport mechanism and the raised tunneling probability of electrons from the excited states of the CNTC back to the source contact could be the reason for the lowered plateau height. These fractional plateaus cannot be explained by a parallel transport through two or more CNT’s because it has been shown that a parallel transport results in an increased plateau height.¹⁶

In Fig. 5 it can also be seen that there are frequencies inside the passband of the IDT’s where no current quantization has been detected (e.g., between $f=472$ MHz and $f=475$ MHz). This is caused by reflected SAW’s from the second unused IDT and has been investigated in detail in Ref. 17. There in agreement with Fig. 3 also no current quantization as a function of rf frequency has been detected.

The following discussion starts with an analysis of the current oscillations presented in Fig. 2. Similar oscillations of the acoustoelectric current have also been detected in AlGaAs/GaAs heterostructures.^{15,18,19} In split-gate-induced one-dimensional channels unintentional quantum dots (QD’s) can be formed accidentally by the potential of impurities. Pronounced current oscillations have been measured close to conduction pinch off in these samples. In Ref. 18 the assumption has been made that the rather complicated charge transport could be dominated by Coulomb-blockade-type effects. This idea has been investigated in more detail in Ref. 15 where also an unintentional QD was present in the induced one-dimensional channel of a GaAlAs/GaAs heterostructure. It has been shown that the potential of the SAW modulates the tunnel barriers of the accidentally confined QD and a SAW-mediated tunneling of electrons through the zero-dimensional electronic states has been proposed. If the SAW wavelength exceeds the length of the confined low-dimensional potential (like sample A with $\lambda_{SAW}=35$ μ m), also, an acousto-electric current of reversed sign has been detected^{18,19} (and in Fig. 2). The piezoelectric potential is supposed to lower both the potential barriers at the entrance and exit of the constriction at the same time. Then an acoustoelectric current with both signs can be measured, depending on the relative position of the electronic states in the constriction to the Fermi levels in the metal contacts.

A continuation of the work of Ref. 15 has been presented recently.²⁰ A QD has been induced deliberately by three independent metallic split gates in a AlGaAs/GaAs heterostructure, and a single-electron transport by SAW’s has been

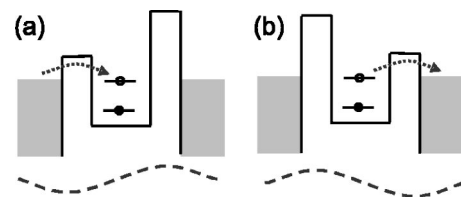


FIG. 6. Schematic model of the transport mechanism. One by one an electron is cycled through the CNTC by the piezoelectric SAW potential (sketched as dashed lines).

demonstrated. The length of the lithographically defined QD was half the wavelength of the SAW, and the transport mechanism is a turnstilelike tunneling of electrons through the QD.

A schematic model of the assumed turnstilelike transport mechanism in conformance with the results presented in Ref. 20 is sketched in Fig. 6. First the piezoelectric potential of the SAW lowers the tunneling barrier of the metal/CNTC contact and an additional electron is tunneling onto the CNTC. Half a period later [see Fig. 6(b)] the exit potential barrier is lowered and the electron is leaving the CNTC towards the drain contacts. This turnstile transport mechanism leads to a quantized current. The presented results of a SAW-mediated SWNT electron pump is in general similar to the theoretical work of a CNT-based parametric electron pump¹²

except the fact that Coulomb repulsion is essential in the turnstile model.

In summary we have realized an acoustoelectric current transport through SWNT's. For larger wavelength the acoustoelectric current oscillates as a function of applied rf power, showing a probing of the low-dimensional electronic states by the potential of the SAW. By decreasing the wavelength of the SAW a quantization of the acoustoelectric current has been detected.

The authors like to thank C. Dupraz and U. Beierlein for their support with the SWNT's. The work on the NT alignment was funded in part by the Bayerische Forschungsförderung under the program ForNano.

*Electronic address: jens.ebbecke@physik.uni-augsburg.de

¹S. Iijima, *Nature (London)* **354**, 56 (1991).

²R. Egger, *Phys. Rev. Lett.* **83**, 5547 (1999).

³M. Bockrath, D. H. Cobden, P. L. McEuen, N. G. Chopra, A. Zettl, A. Thess, and R. E. Smalley, *Science* **275**, 1922 (1997).

⁴S. J. Tans, M. H. Devoret, H. Dai, A. Thess, R. E. Smalley, L. J. Geerligs, and C. Dekker, *Nature (London)* **386**, 474 (1997).

⁵S. J. Tans, M. H. Devoret, R. J. A. Groeneveld, and C. Dekker, *Nature (London)* **394**, 761 (1998).

⁶Z. Yao, H. W. C. Postma, L. Balents, and C. Dekker, *Nature (London)* **402**, 273 (1999).

⁷T. Ida, K. Ishibashi, K. Tsukagoshi, Y. Aoyagi, and B. W. Alphenaar, *Superlattices Microstruct.* **27**, 551 (2000).

⁸M. Suzuki, K. Ishibashi, T. Ida, D. Tsuya, K. Toratani, and Y. Aoyagi, *J. Vac. Sci. Technol. B* **19**, 2770 (2001).

⁹J. W. Park, J. B. Choi, and K.-H. Yoo, *Appl. Phys. Lett.* **81**, 2644 (2002).

¹⁰V. I. Talyanskii, D. S. Novikov, B. D. Simons, and L. S. Levitov, *Phys. Rev. Lett.* **87**, 276802 (2001).

¹¹D. J. Thouless, *Phys. Rev. B* **27**, 6083 (1983).

¹²Y. Wei, J. Wang, H. Guo, and C. Roland, *Phys. Rev. B* **64**,

115321 (2001).

¹³C. J. Strobl, C. Schäfflein, U. Beierlein, J. Ebbecke, and A. Wixforth, *Appl. Phys. Lett.* **85**, 1427 (2004).

¹⁴S. Datta, *Surface Acoustic Wave Devices* (Prentice-Hall, Englewood Cliffs, NJ, 1986).

¹⁵N. E. Fletcher, J. Ebbecke, T. J. B. M. Janssen, F. J. Ahlers, M. Pepper, H. E. Beere, and D. A. Ritchie, *Phys. Rev. B* **68**, 245310 (2003).

¹⁶J. Ebbecke, G. Bastian, M. Blöcker, K. Pierz, and F. J. Ahlers, *Appl. Phys. Lett.* **77**, 2601 (2000).

¹⁷J. Cunningham, V. I. Talyanskii, J. M. Shilton, M. Pepper, M. Y. Simmons, and D. A. Ritchie, *Phys. Rev. B* **60**, 4850 (1999).

¹⁸J. M. Shilton, D. R. Mace, V. I. Talyanskii, Y. Galperin, M. Y. Simmons, M. Pepper, and D. A. Ritchie, *J. Phys.: Condens. Matter* **8**, L337 (1996).

¹⁹V. I. Talyanskii, J. M. Shilton, J. Cunningham, M. Pepper, C. J. B. Ford, C. G. Smith, E. H. Linfield, D. A. Ritchie, and G. A. C. Jones, *Physica B* **249**, 140 (1998).

²⁰J. Ebbecke, N. E. Fletcher, T. J. B. M. Janssen, F. J. Ahlers, M. Pepper, H. E. Beere, and D. A. Ritchie, *Appl. Phys. Lett.* **84**, 4319 (2004).